

A HIGH ENERGY, SMALL PHASE-SPACE VOLUME MUON BEAM *

J. Cox, F. Martin, M. L. Perl, T. H. Tan, W. T. Toner and T. F. Zipf
Stanford Linear Accelerator Center,
Stanford University, Stanford, California

and

W. L. Lakin
High Energy Physics Laboratory
Stanford University, Stanford, California

ABSTRACT

The design and performance of a high-momentum, small phase-space volume muon beam is described. The muons are photoproduced by the bremsstrahlung of electrons incident on a thick target. Pion contamination is reduced to 3×10^{-6} of the muon flux by a 5.5 meter beryllium filter placed immediately after the target. The optical system has two stages of momentum analysis to give an almost dispersion free beam, and a final imaging stage to clean up the tails of the beam distribution. Standard B. N. L. 8Q48 and 18D72 magnets are used throughout. At 10 GeV/c, the beam yields $1.0 \times 10^5 \mu^\pm$ /second in a phase space volume of $3 \times 10^{-3} \text{ cm}^2$ steradians and a momentum band of $\pm 1.5\%$.

(Submitted to Nucl. Instr. and Methods)

* Supported by the U. S. Atomic Energy Commission.

I. INTRODUCTION

At the Stanford Linear Electron Accelerator, muons are produced copiously when an electron beam strikes a thick target. The production process is electromagnetic pair production by the bremsstrahlung of the electrons in the target. The bulk of the production takes place in the first four radiation lengths, and the source of muons has a cross section similar to that of the incident electron beam, of the order of 5 mm \times 5 mm. It is therefore possible to make a muon beam with optical properties similar to those of the high energy beams of strongly interacting particles common at proton accelerators. This may be contrasted with the situation at a proton synchrotron, where the muons are the product of the decay in flight of π -mesons contained in a beam. There, the source of muons has the dimensions of the pion beam, of the order of 10 cms \times 10 cms, and extends over a length of several tens of meters.

In this paper, we describe a beam which has been built at SLAC for a high energy muon scattering experiment. The muons are produced in a water-cooled copper target and then pass through a beryllium filter 5.5 meters long, placed immediately after the target. The π/μ ratio in the beam is reduced to 3×10^{-6} by the filter. Multiple coulomb scattering of the muons in the filter has the effect of making them appear to come from a source with a diameter of about 2.5 cms close to the beginning of the filter. The beam transport system which follows has two stages of momentum analysis to give an almost dispersion free beam, and a final imaging section to clean up the tails of the beam distribution and to shape the beam at the experimental target. With 100 K watts of 17 GeV electrons incident on the production target, the beam yields 1.0×10^5 μ /sec at 10 GeV/c in a momentum band of $\pm 1.5\%$. 90% of the beam is contained within an area of 5 cms \times 10 cms, 99% within an area of 10 cms \times 10 cms.

In Section II we discuss muon production in the target and the target design, in Section III the effects of the filter needed to remove strongly interacting particles, in Section IV the optics of the beam transport system, and in Section V the parameters of the beam and its uses. In Section VI we discuss some possible improvements to the beam.

II. MUON PRODUCTION AND TARGET DESIGN

The principal process by which electrons produce secondary particles in a thick target takes place in two steps. First, an electron radiates in the field of a nucleus. The secondary particles are then photoproduced at another nucleus in the target by the bremsstrahlung. The direct electroproduction reaction $e^- + \text{Nucleus} \rightarrow e^- + \text{Nucleus} + \mu^+ + \mu^-$ can be described as photoproduction by virtual photons whose spectrum is equivalent to the real bremsstrahlung which would be produced by the electron in a target of 0.02 radiation lengths.¹ It can therefore be neglected. The calculation of the muon yield from a thick target involves the integration of the Bethe-Heitler cross section for the pair production over the thick target bremsstrahlung spectrum, taking account of the nuclear form factor and of pair production from individual nucleons. These calculations have been made by Tsai and Whitis.^{2, 3} Some results of their calculations for 18 GeV electrons incident on a 10 radiation length copper target are shown in Figs. 1 and 2. In Fig. 1, the muon flux relative to the flux at 0° is plotted as a function of angle, with the angle in units of m_μ/E_μ . Multiple coulomb scattering in the target has not been included. In the case of 4, 8 and 12 GeV/c muons, the points lie very closely on a common curve. For 15 and 17 GeV/c muons, the fluxes at large angles are suppressed. Also shown in the figure is the function $1/\left(1 + \left(\frac{\theta}{\alpha}\right)^2\right)^2$,

and a gaussian, $\exp \left\{ -\frac{1}{2} \left(\frac{\theta}{0.57\alpha} \right)^2 \right\}$, chosen so as to fit the common curve at 0° and at the half maximum point. The first gives an overestimate, the second an underestimate of the large angle production. For the $1/\left(1 + \left(\frac{\theta}{\alpha}\right)^2\right)^2$ distribution, the total flux is $\pi(m_\mu/E_\mu)^2$ times the flux at 0° , and half of this is contained within an angle of m_μ/E_μ . For a 10.5 GeV/c muon, m_μ/E_μ is 10 mrads., an angle typical of the acceptance of a high energy beam transport system using conventional 8" bore quadrupoles. We can therefore expect to capture a significant fraction of all muons produced into the beam. Figure 2 is a plot versus muon momentum of the flux at 0° per steradian percent $\delta p/p$ per incident 18 GeV electron, and of the total production calculated from the 0° flux. The total muon production at 10 GeV/c for 3.5×10^{13} electrons/second (100 Kwatts of beam power) is $8.7 \times 10^5 \mu/\text{sec}/\% \delta p/p$. Therefore, the production target must be designed to dissipate large amounts of power, if we are to have an intense beam of muons. The muon yield from a thick target depends very little on the target material. However, pions are also produced. The pion production process is a nuclear interaction of the bremsstrahlung with a cross section which is roughly proportional to A. Therefore, the number of grams/cm² per radiation length should be kept small, particularly in the first few radiation lengths, where particle production is a maximum. These considerations make a water-cooled copper target an obvious choice. Gold would be better still. A simplified diagram of the target is shown in Fig. 3. Ten radiation lengths is sufficient to absorb about 70% of the power in the electron beam, and to diffuse the cascade so that its diameter when it leaves the target is ~ 3 cms. The beam power per unit area is then sufficiently small to be handled in the beryllium filter which follows.

III. PION FILTER

A. Pion Contamination

Some preliminary measurements showed that strongly interacting particles, mostly pions, are produced in the copper at the rate of approximately one for every two muons. The interaction cross sections for pions and muons differ by more than three orders of magnitude. To reduce the contamination of pion induced events in an experiment to less than one percent, it is, therefore, necessary to attenuate the strongly interacting particles by a factor of more than $\times 10^5$, the precise value depending upon the particular experiment. More than 11 attenuation lengths of filter are required. The filter is placed immediately after the production target so as to keep the effects of coulomb scattering of the muons, discussed later, to a minimum. All forward produced strongly interacting particles make a cascade in the filter and we must estimate the number which emerge relative to muons of the same energy.

Studies have been made⁴ of the attenuation of monoenergetic protons in shielding material. Measurements of the particle flux as a function of depth show that, at first, the flux of particles increases. Then, after about two mean free paths, it begins to be attenuated exponentially. The conditions in the present case are quite different, although the qualitative behaviour should be similar, and so measurements of the pion flux and attenuation were made in a region where it was expected to be already exponential. A schematic diagram of the apparatus used is shown in Fig. 4. The incident beam is defined by counters 1, 2, and 3. They are followed by a four gap thin plate spark chamber, a spark chamber with nine 2.5 cm thick iron plates, an iron absorber 1 meter thick and anticoincidence counters 4 and 5. The anticoincidence counters were made big enough so that multiple-scattered muons, or muons which had interacted in the iron would still be registered. About

two meters upstream of the spark chambers, four radiation lengths of lead were placed in the beam, so that electrons from muon decay would produce a characteristically spread out shower in the first spark chamber. Electrons from the target were reduced to a negligibly low level by placing a filter of two radiation lengths of lead at the first focus in the beam. This technique has been described already.⁵ The signal $1\ 2\ 3\ \bar{4}\ \bar{5}$ was used to trigger the spark chambers. Almost all pions would give a trigger signal and some definite proportion of them would give a visible interaction in the thick plate spark chamber. The rest would look like muons. Measurements were made with filter lengths of 2.14, 3.35 and 4.88 meters of Be. With 2.14 meters of Be, the trigger rate was almost entirely due to pions, and this rate gave the flux of pions directly. From the pictures, the fraction of pions which gave a visible interaction in the thick plate chamber was determined. With 3.35 meters of Be, about 30% of the pictures had electron-like events. The attenuation of the pion flux produced by the additional 1.2 meters of Be was determined by the relative number of pictures with pion-like interactions in the two cases. Counter measurements were made with a 4.88 meter filter. In this case, the trigger rate was almost entirely due to electrons, and was consistent with the number of electron-like events observed with 3.35 meters of Be. The results of this study are as follows: With 3.35 meters of Be the π/μ ratio is $(3.2 \pm 0.4) 10^{-4}$, and the attenuation length of Be is $0.47 \begin{smallmatrix} +.03 \\ -.02 \end{smallmatrix}$ meters. In the geometry we used, $(2.6 \pm 0.2) 10^{-4}$ electrons/ μ from μ decay were counted. These measurements were made with 8 GeV/c μ^- from 16 GeV/c e^- . With the 2.14 meter filter, measurements were made at other momenta. They showed that above 4 GeV/c the π/μ ratio did not change significantly with momentum. Therefore, the change in momentum due to dE/dx loss in the filter does not influence the π/μ ratio. Our present filter is 5.5 meters of Be, giving a value of $(0.30 \begin{smallmatrix} +.16 \\ -.09 \end{smallmatrix}) \times 10^{-5}$ π/μ in

the beam. This is adequate for the experiments which are at present being carried out, since they incorporate a steel shield through which the scattered muons must pass, which gives a further rejection against pion-induced events.

B. Electron Contamination

The primary electrons incident on the target very rapidly lose their energy by bremsstrahlung. The bremsstrahlung is then attenuated at a rate of $e^{-7t/9x_0}$. Conversion of these photons in the last radiation length of the filter leads to a contamination of electrons in the beam. This may be estimated from the results of Ref. 2. With a total thickness of target and filter of 25.5 radiation lengths, the electron contamination is approximately 1% of the muon flux.

C. Multiple Coulomb Scattering. Choice of Beryllium

The source of muons is characterized by the size of the incident electron beam and the production angular distribution folded in with the multiple coulomb scattering in the ten radiation length target. The muons then undergo further multiple coulomb scattering in the filter. Since it extends over a finite distance from the source, the scattering in the filter broadens the apparent source seen by the subsequent beam transport elements, and shifts its apparent location downstream. It is clearly advantageous to place the filter as close as possible to the production target, or to a plane in which the target is imaged. The effect of the filter on the distribution in phase space of the muons can be calculated in a straightforward manner. We project all angles and displacements onto a plane containing the beam. Let θ_{prod} be the RMS projected production angle (radians) and θ_{scatt} the RMS projected angle of scattering in the target. Then

$$\theta_s = \sqrt{\theta_{\text{prod}}^2 + \theta_{\text{scatt}}^2} = \text{RMS projected angle of muons emerging from the target.}$$

We have seen in Section II that a gaussian approximation to the flux at

production gives an underestimate of the large angle flux, and $1/\left(1 + \left(\frac{\theta}{\alpha}\right)^2\right)^2$ gives an overestimate. We take the mean of the values of the RMS projected angle from these two distributions as a reasonable approximation for the treatment which follows. Its value is $\sqrt{\theta_{\text{prod}}^2} = 0.8 \text{ m}_{\mu}/E_{\mu}$ radians. The energy dependence is the same as for coulomb scattering, and it is instructive to calculate the thickness of scatterer which would give an RMS projected scattering angle of the same size. It is $(0.084/0.015)^2 = 31$ radiation lengths. The 8 or so radiation lengths of copper traversed by the muons after they are produced do not, therefore, seriously reduce the fraction of muons which can be captured in the beam transport system. We can write $\theta_S = \frac{.015}{p} \sqrt{39}$ radians, with p in GeV/c. The target is compact enough so that it is effectively located at the source and does not appreciably broaden the beam. The filter is much less compact and does have a serious effect on the phase space occupied by the muons. Let θ_R be the RMS projected angle of scattering in the filter, and Z the length of the filter, in meters. Starting from the distribution function $P(Z, y, \theta)$,⁶ which is the probability that a particle incident on the filter along the Z axis has a displacement y and angle θ at depth Z, and folding in a gaussian source distribution and emittance, it can be shown (after some tedious algebra) that the muons appear to come from a source a distance $L = Z/\left(2\left(1 + \theta_S^2/\theta_R^2\right)\right)$ meters downstream of the target, with an RMS projected angle $\theta_{\text{RMS}} = \sqrt{\theta_S^2 + \theta_R^2}$.

The apparent source has a width

$$\sigma = \sqrt{\sigma_S^2 + \frac{\theta_R^2 Z^2}{12} \left(\frac{\theta_R^2 + 4\theta_S^2}{\theta_R^2 + \theta_S^2} \right)},$$

where σ_S is the RMS projected width of the incident electron beam. The density of particles per unit area of θ, y phase space before the filter is proportional to $1/(\theta_S \sigma_S)$ and after the filter to $1/(\theta_{\text{RMS}} \sigma)$.

The dilution due to the filter is thus

$$D = \sqrt{1 + \frac{\theta_R^2}{\theta_S^2}} \sqrt{1 + \frac{\theta_R^2 Z^2}{12 \sigma_S^2} \left(\frac{\theta_R^2 + 4\theta_S^2}{\theta_R^2 + \theta_S^2} \right)}$$

In the four-dimensional phase-space y, θ, x, ϕ , the dilution is just D^2 . In the derivation of these expressions, the energy loss of the muons in the filter has been neglected. This may be taken into account exactly in the case of the angles by using the momentum at production to calculate θ_S , and by using the square root of the product of the momenta before and after the filter as the momentum in the expression

$$\theta_R = \frac{.015}{p} \sqrt{\frac{Z}{x_0}} \quad .$$

Substitution of these values in the formulae for σ , L and D^2 still does not allow for the shift downstream of the scattering. To take this into account approximately, we observe that the point in the filter at which the mean square angle of scattering reaches half its final value is $Z/2$ in the case of no energy loss, and $(Z/2)(1 - \Delta p/2p_0)^{-1}$ when the initial momentum is p_0 and the final momentum $p_0 - \Delta p$. We use this value for $Z/2$ in the formula for L , and $Z(1 - \Delta p/2p_0)^{-1}$ for Z in the expressions for σ and D^2 , together with the corrected angles θ_S and θ_R . In Table I, values of D^2 are given for various materials with a length containing the same number of collision lengths as our 5.5 meter Be filter. Beryllium is clearly favored. Values are also given for θ_S , θ_{RMS} , and L . Table II gives values of D^2 and σ for Be as a function of the length of the filter. The advantages in keeping the length of the filter to a minimum are obvious.

D. Mechanical Design of the Filter

The filter is made of vacuum cast cylinders of Be, each 18 cm diameter and 30 cm long. They are encased in a 30 cm \times 30 cms square casting of lead, made

up in 0.6 meter, 1.2 meter, and 1.8 meter sections. End windows of aluminum seal the beryllium. The first 0.3 meters of the filter is attached to the target. The beryllium is water-cooled to remove the power of up to 30 Kwatts contained in the electron-photon cascade emerging from the target.

IV. OPTICAL DESIGN

The floor layout of the beam and particle trajectories through the system are shown in Figs. 5 and 6. The effective source of the muons is a short distance downstream of the beginning of the target, as discussed in Section III above. The beam is at 0° to the direction of the incident electrons. The first two lenses, Q1 and Q2, form an image of the source in both planes at the first slit, S1. Lead collimators in these lenses define the aperture of the beam. The magnification of the source at S1 is $\times 1.08$ in the horizontal plane and $\times 4.1$ in the vertical. Bending magnets D1, D2, and D3 deflect the beam through a total angle of 12.9° , to give a dispersion at S1 of 3.2 cms per percent. Q3 and Q4 are field lenses. Q5 and Q6, together with D4, D5 and D6, give an almost dispersion free image of the source in both planes at S2. The magnification of the source at S2 is $\times 0.93$ in the horizontal plane and $\times 3.66$ in the vertical. Q7 and Q8 are field lenses. Q9 and Q10 can be varied to produce different beam configurations in the experimental area. They are usually set to make an image in both planes of the source at the downstream end of the hydrogen target used in the muon scattering experiment. The basic optical parameters of the beam are listed in Table III. The effects of chromatic aberrations on the beam are negligible. The most important features of the beam design are as follows:

1. The beryllium filter is placed as close to the production target as possible.
2. The aperture of the beam is defined very early, at the first lenses. The

beam thus defined is kept well inside the aperture of all subsequent magnets, lenses and collimators.

3. The vertical extent of the effective source is redefined by S1. It is 10 cms high. The vertical opening of S2 is made significantly bigger than the image of S1 at S2, so that the main beam is not touched by S2.

4. The horizontal extent of the effective source is determined by the source dimensions, modified by coulomb scattering in the Be filter, and by S2. S2 is made wider than the beam image at this point so that, again, only the tail of the beam can be scattered here.

5. The final beam is re-formed after S2 by Q7, Q8, Q9 and Q10, so that the scattering target of the experiment is well removed from any heavy collimators.

The definition of the beam aperture and images is determined exclusively by multiple coulomb scattering and a small amount of dE/dx loss in the collimators. The heavy shielding shown around the beam is to protect against muons which do not pass through the optical channel by bringing them to rest. The small volume in phase space occupied by the beam, and the fact that the collimators are placed where the angular spread of particles in the beam is small, contribute to the effectiveness of the coulomb scattering. Slits S1 and S2 are made of steel and are each 1 meter long. They form closed iron circuits around the beam and can be magnetized so as to deflect any particle entering the steel further from the beam. In 1 meter of iron at 15 KG, particles are deflected by the field through 4 times the RMS projected angle of multiple scattering. Tests showed that the effect of magnetizing S1 was not measurable. On the other hand, magnetizing S2 reduced the background trigger rate in the muon experiment by a factor of two.

V. PERFORMANCE OF THE BEAM

A. Beam Profiles; Momentum Bite

The intensity distribution of muons at the effective source, discussed in Section III, is approximately gaussian. The width of this distribution will determine the momentum resolution of the beam. If we neglect chromatic aberrations, the displacement in the horizontal plane of a trajectory at S1 is given by

$$x_1 = M_{01} x_0 + D\delta p/p$$

where x_0 is the displacement at the source, M_{01} is the magnification of the source at S1, D is the dispersion and δp is the departure from the nominal beam momentum, p . For an infinitesimal slit, $x_1 = \text{constant}$, and the momentum distribution of the transmitted beam will have the shape of the intensity distribution at the source, suitably scaled. As the width of the slit increases, the width of the momentum distribution increases. When S1 is wide enough to pass the whole of the source image at the reference momentum, the full width at half maximum intensity of the momentum distribution becomes $\frac{W}{D}$. Typical distributions are shown in Fig. 7(b).

At S2, the beam is sufficiently dispersion free that we can write $x_2 = M_{02}x_0$, independently of the momentum of the particles. Some reflection should be sufficient to convince the reader that the shape of the intensity distribution in the horizontal plane at S2 is independent of the width of the momentum slit, and is the same as that of the source distribution, scaled by the magnification. We may therefore deduce the shape of the effective source distribution and of the momentum distribution from horizontal scans of the beam image at S2. A point at S2 corresponds to a point at the source. The momentum distribution of particles at one point in the image of S2, therefore, corresponds to the momentum distribution which would be obtained with a point source. It is a square distribution

with a full width of $\frac{W}{D}$. At the third focus, F3, the intensity distribution and momentum distribution will be the same as at S2, when account is taken of the magnification, except that the particles in the tails of the distribution are scattered and bent out of the beam by S2. Figure 7(a) shows horizontal beam profiles at S2 taken with S1 set at ± 5 cm wide ($\pm 1.5\% \delta p/p$). Momentum distributions deduced from these profiles are shown in Fig. 7(b). In the vertical plane, the magnification at S1 is $\sim \times 4$, and there is no dispersion, so S1 re-defines the source for the subsequent beam system. Figure 8 is a vertical scan of the beam at S2. The solid line represents the data. The dashed curve is a horizontal beam profile taken under the same conditions, scaled to the appropriate magnification. The limits set by S1 and S2 are also shown. The effectiveness of the 1 meter of iron in S1 in removing muons from the beam is clear. The beam shape in the vertical scan is almost independent of momentum, although the horizontal width increases significantly as the beam momentum is reduced. Figures 9(a) and (b) are horizontal and vertical beam profiles at the third focus for 12 GeV/c muons.

B. Background Particles and Shielding

1. Shielding from low energy photons, neutrons, etc.

The production target is in the B target room at SLAC. Along the beam line it is followed by the 5.5 meter beryllium filter. This is set in a steel wall, the upstream part of which is 3.7 meters thick and completely shuts off the target room from the End Station Building. This is followed by a further 3.7 meters of steel 1.8 meters wide by 1.2 meters high with the beam channel down the center. The radiation background in the end station building is low enough to operate scintillation counters in the beam about 10 meters downstream of this shield quite satisfactorily. In view of the 5×10^{-4} duty cycle, this is quite a low level. The experimental area is further shielded by the walls of the End Station Building which are of concrete.

At the position of our experiment, 90 meters from the target room, we operate a bank of counters with an area of 2 square meters without difficulty. We do see evidence of slow neutrons in the few MeV range, but these come after the end of the 1.4 μ sec beam pulse.

2. Shielding against muons

Muon production is so sharply peaked in the forward direction that the bulk of all muons produced pass down the beam channel through Q1 and Q2 to the first bend. There, off-momentum muons are deflected to either side. These bending magnets are followed by a heavy shield long enough to stop muons of up to 12 GeV/c momentum. Muons produced at large angles are of low momentum. The angle-energy relation of muon production works with the range-energy relation to make the maximum lateral excursion of muons in the shielding small and independent of momentum.

In the last leg of the beam there is another 12 meters of steel around the beam to stop or scatter any muons which remain outside the optical channel. The shield shown just downstream of Q4 was installed later, and did not appear to change the residual background appreciably. The only shielding added after the initial design which did affect the background was the steel at the side of the beam at Q9 and above the beam just following D6. Muons at large distances from the beam were removed almost completely. The shielding around the beam is so effective that the 2.5 meter \times 1.4 meter spark chambers of the muon experiment show more background particles coming from a collimator 900 meters upstream of the muon production target at an angle of the order of 10^0 to the direction of the muon beam than they show particles produced in the target room.

C. Beam Halo

The combination of the very low cross section for muon interactions (\sim a few μ barns for the inelastic cross section) and the 5×10^{-4} duty cycle makes the beam

halo one of the most critical features of the performance. At present, the beam halo is sufficiently low for the experiments which are being carried out. About 1% of the total muon flux is in a halo lying just outside the beam envelope, but within a 9 cm radius circle, another 1% or so lies beyond this, extending to a radius of about 75 cms.

With the evidence of Fig. 8 of how well a short collimator can define a muon beam, it is clear that the addition of a further stage of beam transport – or possibly just a bend in the last section – could effect a significant reduction in the halo. Ultimately, a muon beam should be better in this respect than a pion beam, since the muons decay only infrequently, and into electrons which are easily distinguishable.

D. Summary of Beam Parameters

The most important features of the beam performance are summarized in Table IV. The muon flux peaks at between 8 and 10 GeV/c for 16 GeV electrons incident. The size of the beam shrinks as the momentum is increased. The 0° beam transport system can also be used to give a pion beam, as described in Ref. 5, if the copper target and beryllium filter are removed and replaced by a thin (~ 1 to 2 radiation lengths) beryllium target.

VI. POSSIBLE IMPROVEMENTS

In the muon-proton scattering experiment which we are performing at present, we are not limited by the beam quality per se, but by knock on electrons produced in the hydrogen target by the beam muons themselves. The first spark chamber in the experiment is 1.3 meters downstream from the end of the liquid hydrogen target. The beam passes through a 12 cm diameter hole in the chamber plates. With the hydrogen target empty, we can run up to 250 muons/ $1.4 \mu\text{sec}$

pulse before stray tracks in the chamber become a serious worry. With the target full, the limit is in the region of 150 muons/pulse, despite the fact that we have a 2 kg-meter magnet between the target and chambers to sweep out the δ -ray background.

It is nevertheless interesting to consider what improvements could be made to increase the flux of the beam and decrease the halo, since future experiments might not be limited in the same way.

1. The present beam is limited in flux by power dissipation in the production target to 100 Kwatts. The Stanford Linear Electron Accelerator can run at present with an average power of 300 Kwatts, and up to 1 Mwatt may be attained in the future. Using more power would entail a redesign of the beam dump and of the Be filter for more efficient cooling. The muon flux would, of course, increase linearly with beam current.

2. The addition of another focusing stage at the beginning of the beam, as shown in Fig. 10, would bring the following improvements. (a) The beam source could be re-defined in both planes at a slit after it had passed through the bulk of the Be filter. The horizontal beam profile would then fall off as steeply as the vertical. (b) The beryllium filter could be split in three, so that the scattering would all take place very close to the target, or its image. The effective source size, and therefore the phase-space volume occupied by the muons, would be smaller by a factor of about 9 at 10 GeV/c. A factor of about 2 increase in muon flux would be obtained at 10 GeV/c, somewhat more at lower momenta. (c) With the smaller phase-space volume occupied by the beam muons, collimation and removal of halo muons should be more effective.

With a 300 Kwatt beam on the target and the improvements in (2) above, we estimate that the muon flux would increase by a factor of about 6 at 10 GeV/c, and

the phase-space volume of the beam decrease by a factor of about 9. The beam halo would also improve, but the amount is difficult to estimate. Adding another stage at the end of the beam, or incorporating a small bend in the last stage, would cut it by an order of magnitude.

ACKNOWLEDGEMENTS

The muon beam was the first high energy particle beam to be constructed at SLAC; all magnets, power supplies, control systems and installation techniques were new and untried. The success with which the beam was installed and commissioned is a tribute to the work of many people too numerous to mention individually. We would like to thank all the engineers, surveyors, riggers, electricians and others in the technical division whose work went into the construction of the beam. We would like in particular to thank Mr. R. Vetterlein who did the engineering design and supervised the installation of the beam, and Mr. C. A. Harris and his technicians for their tireless work with the power supplies.

We are grateful to Dr. Y. S. Tsai and Mr. V. Whitis for permission to use their unpublished data on muon production and for many useful conversations.

REFERENCES

1. W. K. H. Panofsky, C. M. Newton and G. B. Yodh, Phys. Rev. 98, 751, 1955.
2. Y. S. Tsai and V. Whitis, Phys. Rev. 149, 1248, 1966.
3. Y. S. Tsai and V. Whitis, SLAC Users Handbook, Part D (unpublished) and private communication.
4. CERN Shielding Studies, Nucl. Instr. and Methods 32, 45, 1965.
5. A. Barna et al., Phys. Rev. Letters 18, 360, 1967.
6. B. Rossi, High Energy Particles (Prentice-Hall, 1952), p. 71.

TABLE I

Properties of Filters Made of Different Materials

Material	Length*			Values for 10 GeV/c μ 's			
	Collision lengths	Radiation lengths	Meters	Energy loss GeV	Displacement of Apparent Source (meters)	σ (cms)	D^2
Li	18	11.5	17.0	1.5	2.3	4.5	108.0
Be	18	15.5	5.4	1.6	0.9	1.7	16.4
C	18	25.6	7.2	1.9	1.7	2.6	50.0
Al	18	59.0	5.3	2.3	1.9	2.6	75.0
Cu	18	158.0	2.1	2.7	1.0	1.5	55.0
U	18	390.0	1.4	3.2	0.7	1.4	111.0

σ_s = RMS width of incident electron beam, taken as 0.5 cms.

σ is the RMS width of the apparent source of muons.

D^2 is the factor by which the density in 4-dimensional phase space of the muons is reduced by the filter.

* Data from UCRL-8030

TABLE II

Properties of Be Filters as Function of Length and Muon Momentum

Momentum of muons	Length*			π/μ ratio	Energy loss GeV	σ (cms)	D ²
	Collision lengths	Rad. lengths	Meters				
12	18	15.5	5.4	$3 \cdot 10^{-6}$	1.6	1.4	8.9
8						2.1	25.0
4						3.9	95.0
10	22	19.0	6.6	$0.24 \cdot 10^{-6}$	1.9	2.2	30.0
	18	15.5	5.4	$3 \cdot 10^{-6}$	1.6	1.7	16.4
	14	12.0	4.2	$38 \cdot 10^{-6}$	1.2	1.2	8.2

*Data from UCRL 8030

TABLE III

Optical Parameters of Beam

Position	Distance from Target	Horizontal Plane		Vertical Plane
		Magnification	Dispersion	Magnification
S1: Momentum Slit	30 meters	1.08	3.25 cm/%	4.1
S2: Second Focus	65 meters	0.93	.45 cm/%	3.7
F3: Third Focus	88 meters	0.72	.35 cm/%	3.4

TABLE IV

Beam Performance

Momentum	12.0	10.0	6.0	3.0	GeV/c
Momentum Bite	$\pm 1.5\%$	$\pm 1.5\%$	$\pm 1.5\%$	$\sim \pm 1.5\%$	
Flux for 100 KWatts of 16 GeV electrons	0.31×10^5	0.8×10^5	0.82×10^5	0.29×10^5	μ per second
Flux for 100 KWatts of 17 GeV electrons	0.59×10^5	1.03×10^5	-	-	"
Vertical beam width at S2 Full width at 10% intensity	9.5	9.8	9.8	10.6	cms
Horizontal beam width at S2 Full width at 50% intensity	2.9	3.2	5.4	4.8	"
Full width at 10% intensity	5.3	5.9	8.8	10.9	"
Vertical beam width at F3 Full width at 10% intensity	9.8	10.0	-	-	"
Horizontal beam width at F3 Full width at 50% intensity	2.4	3.0	-	-	"
Full width at 10% intensity	4.4	5.1	-	-	"

FIGURE CAPTIONS

1. Muon production by 18 GeV electrons in a 10 radiation length target as a function of angle. The production angle is in units of $\alpha = m_{\mu}/E_{\mu}$.
 - (a) Common curve for $p_{\mu} \leq 12$ GeV/c.
 - (b) $p_{\mu} = 15$ GeV/c.
 - (c) $p_{\mu} = 17$ GeV/c.
 - (d) $\left[1 + (\theta/\alpha)^2\right]^{-2}$.
 - (e) $\exp\left\{-1/2\left(\frac{\theta}{.57\alpha}\right)^2\right\}$.
2. Muon production by 18 GeV electrons in a 10 radiation length target as a function of momentum. The lower curve (left hand scale) is the flux at 0° . The upper curve (right hand scale) is the lower curve multiplied by $\pi\left(\frac{m_{\mu}}{E_{\mu}}\right)^2$, and represents approximately the total muon flux.
3. Schematic diagram of water-cooled production target.
4. Schematic diagram of arrangement used to measure π/μ ratio.
5. Floor layout of muon beam.
6. Particle trajectories and beam envelopes. In the horizontal plane the beam envelope is approximately that of the 10 GeV/c beam with a $\pm 1.5\%$ momentum bite.
7. (a) Horizontal beam profiles at the second focus. The ordinate is counts in a $.63 \text{ cm} \times .63 \text{ cm}$ counter normalized to the same flux of electrons on the production target for each curve.
 - (b) Momentum distribution in muon beam deduced from the profiles of Fig. 7(a).
8. Vertical beam profile at the second focus for 12 GeV/c muons (solid curve). The $.63 \text{ cm}$ counter width has not been unfolded. The dashed curve is a horizontal beam profile taken with the same beam conditions, with the abscissa expanded by a factor of 4. The limits set by S1 and S2 are indicated.

9. (a) Horizontal beam profile at the third focus for 12 GeV/c muons.
(b) Vertical profile at the third focus for 12 GeV/c muons.
10. (a) Present arrangement of production target and beryllium filter.
(b) Possible arrangement of production target and filter using a quadrupole doublet to allow the filter to be concentrated at an image plane and to enable the source of muons to be re-defined.

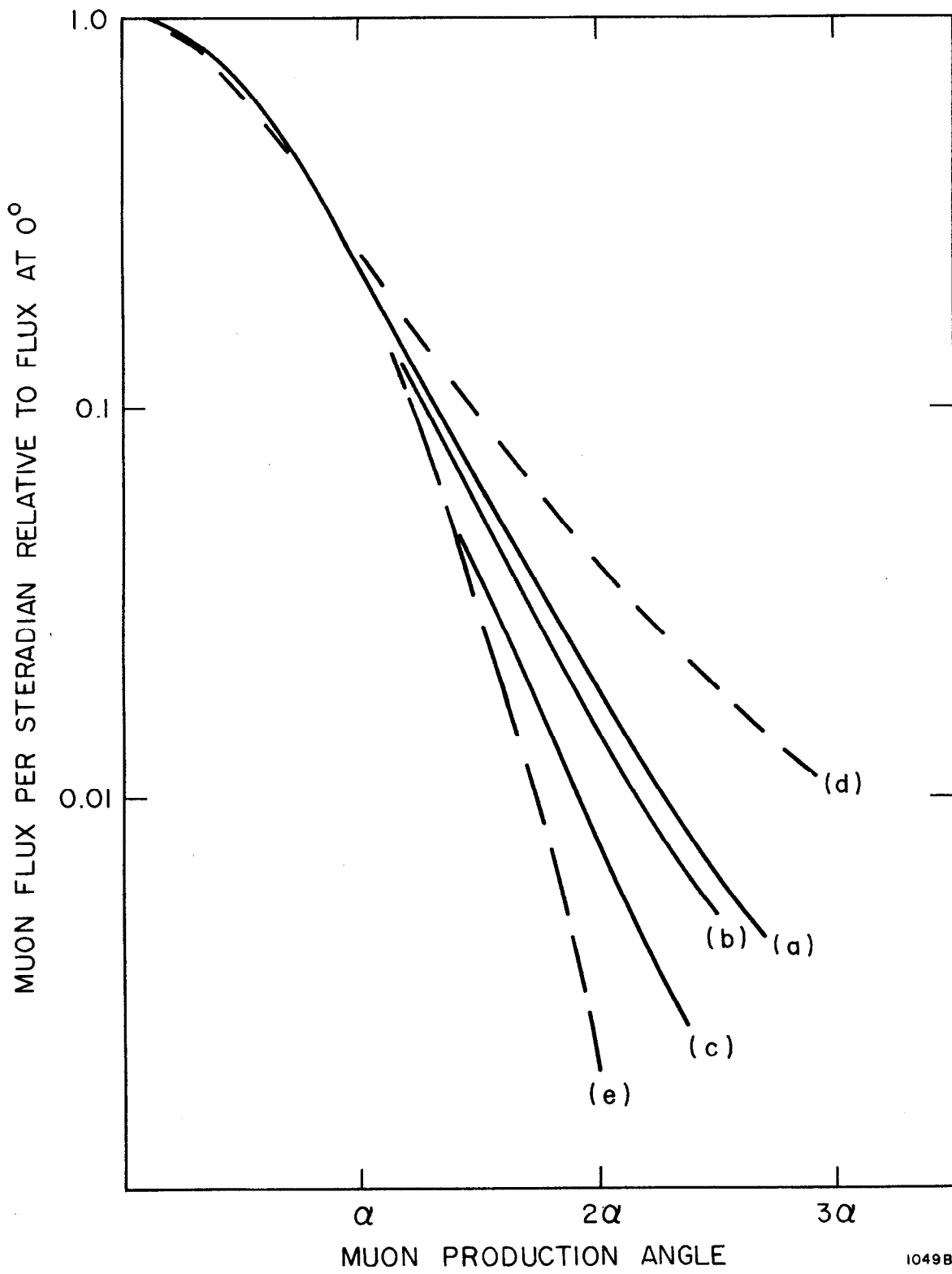
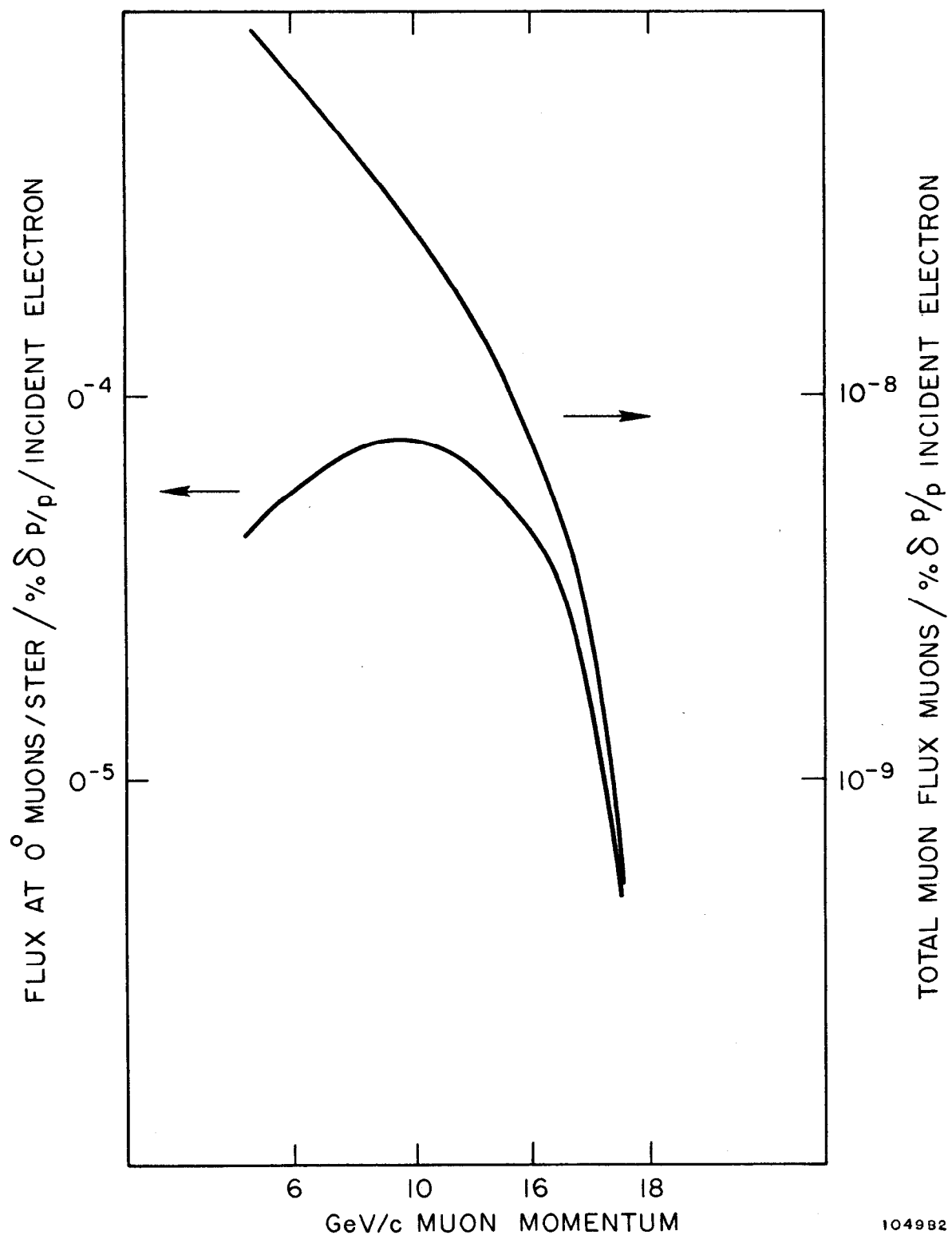
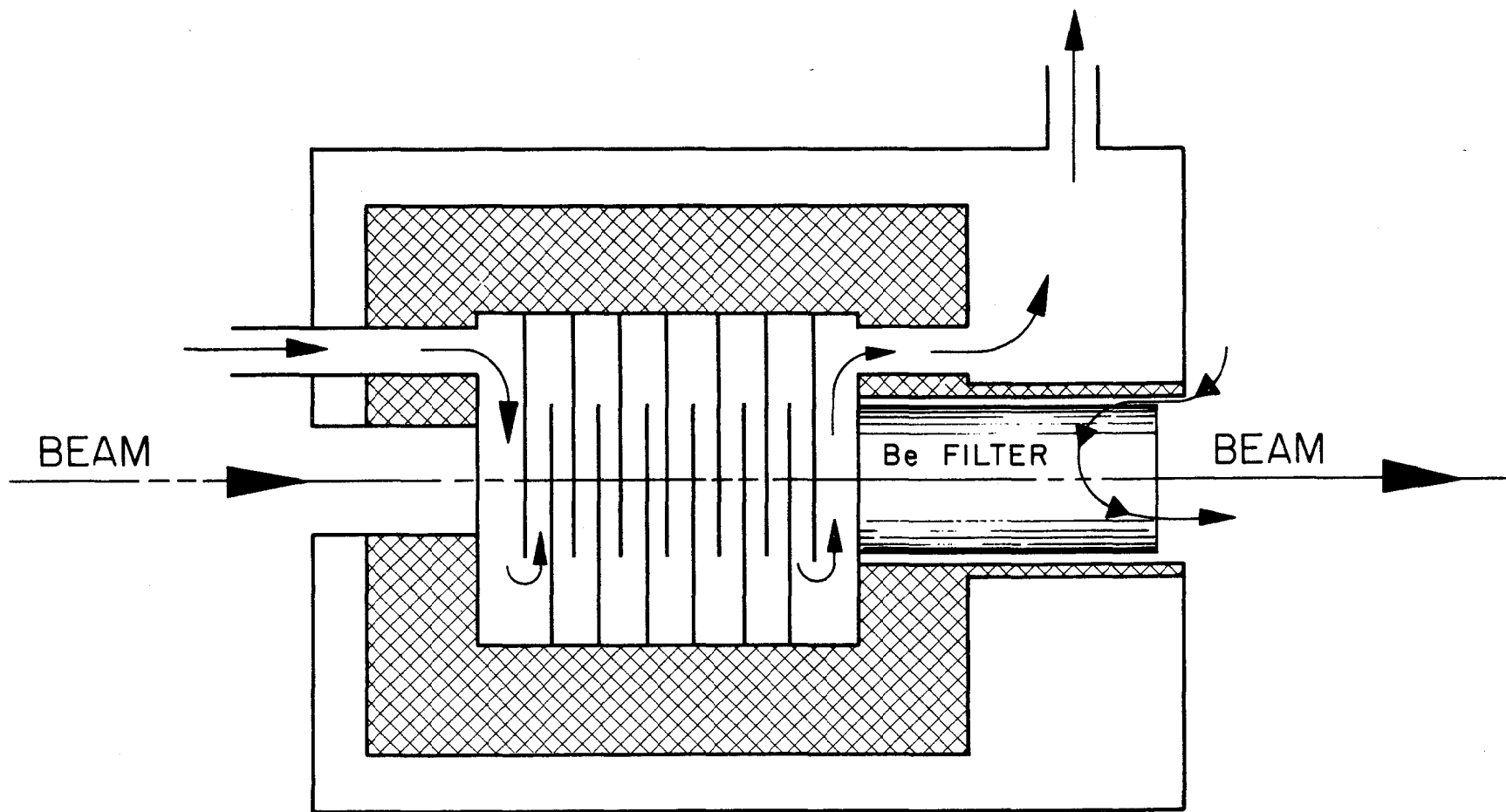


Fig. 1



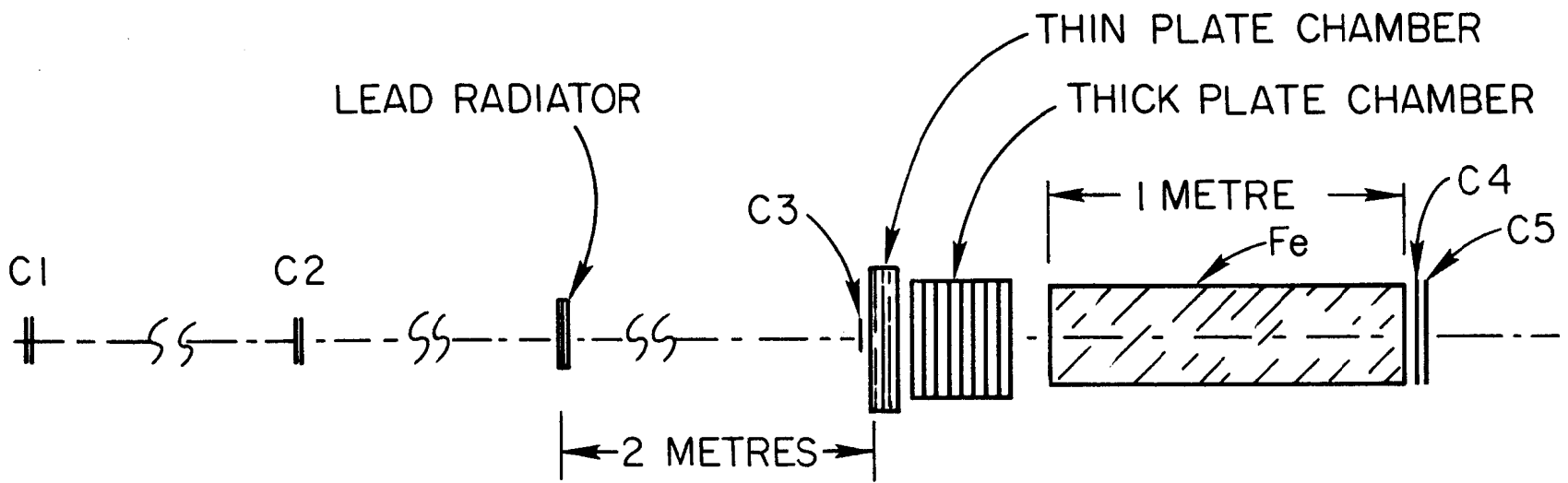
104982

Fig. 2



104989

Fig. 3



1049A3

Fig. 4

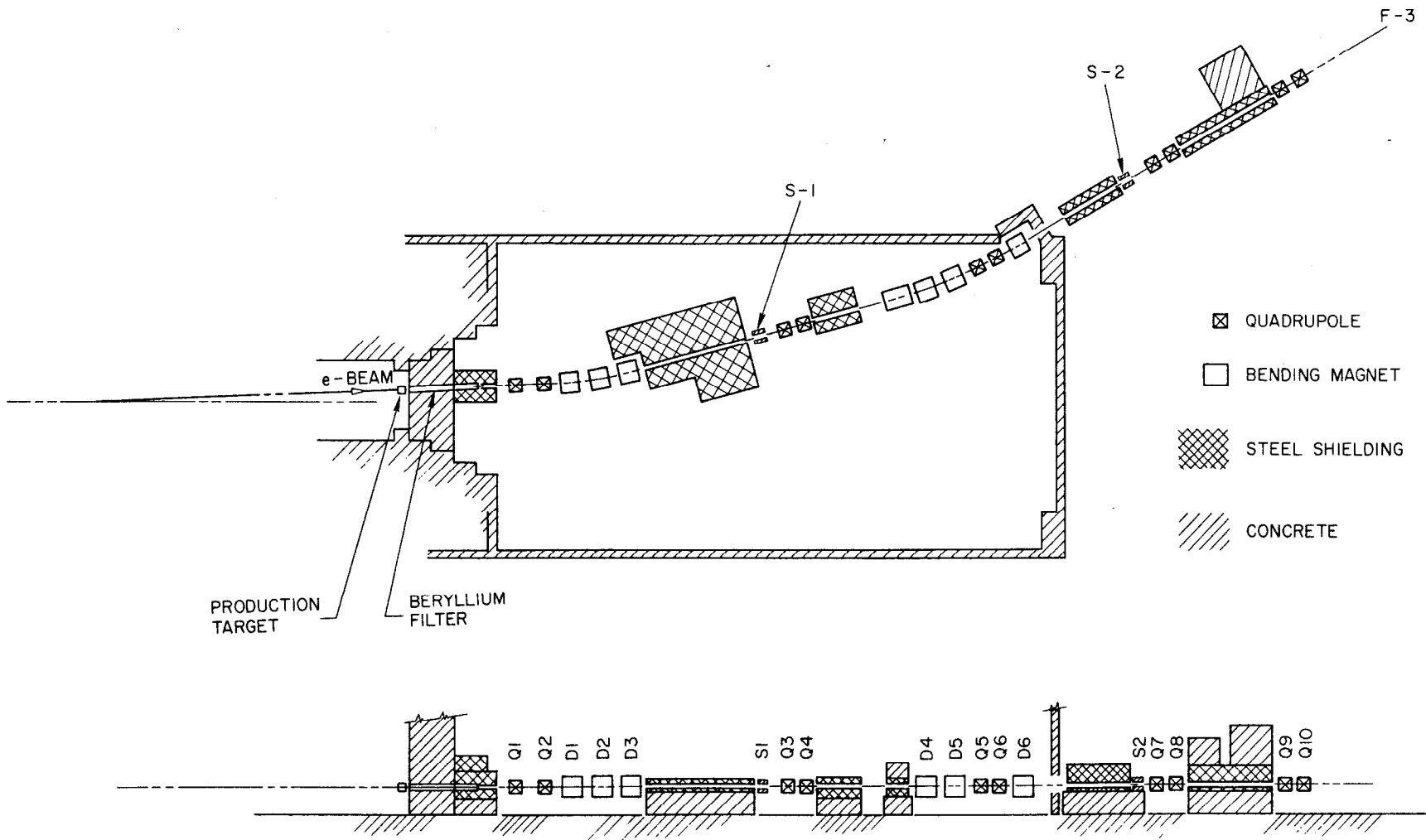
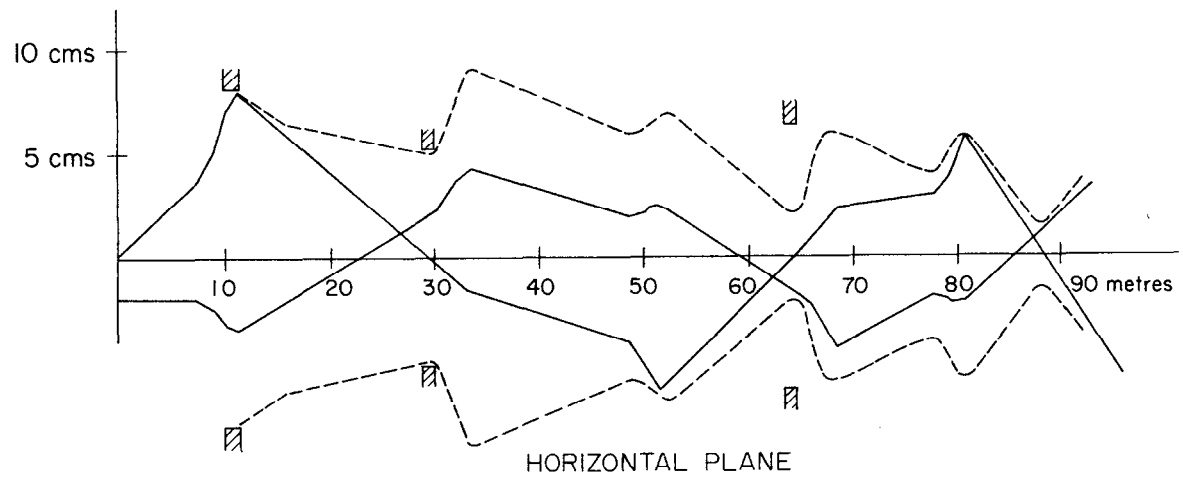
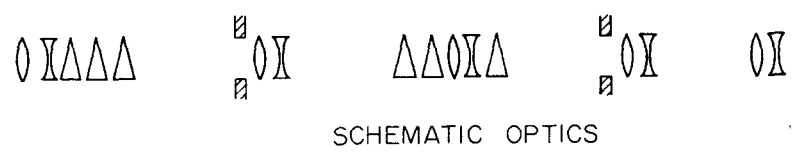
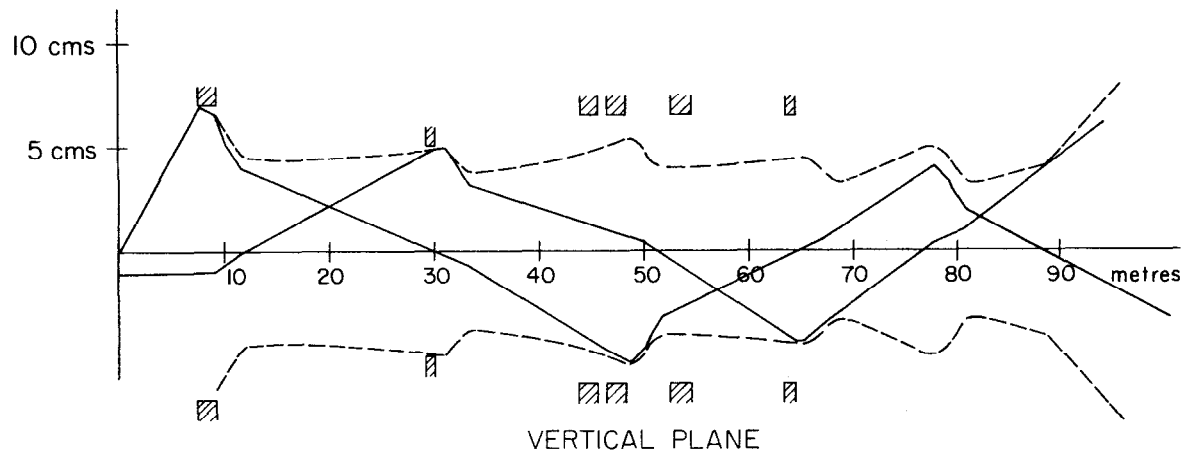


Fig. 5



- | | | | |
|---|---|-----|----------------------|
| — | TRAJECTORIES | --- | ENVELOPES |
| ⊖ | 8Q48 QUADRUPOLE FOCUSING
IN VERTICAL PLANE | △ | 18D72 BENDING MAGNET |
| ⊗ | 8Q48 QUADRUPOLE DEFOCUSING
IN VERTICAL PLANE | ▧ | COLLIMATOR |

1049C6

Fig. 6

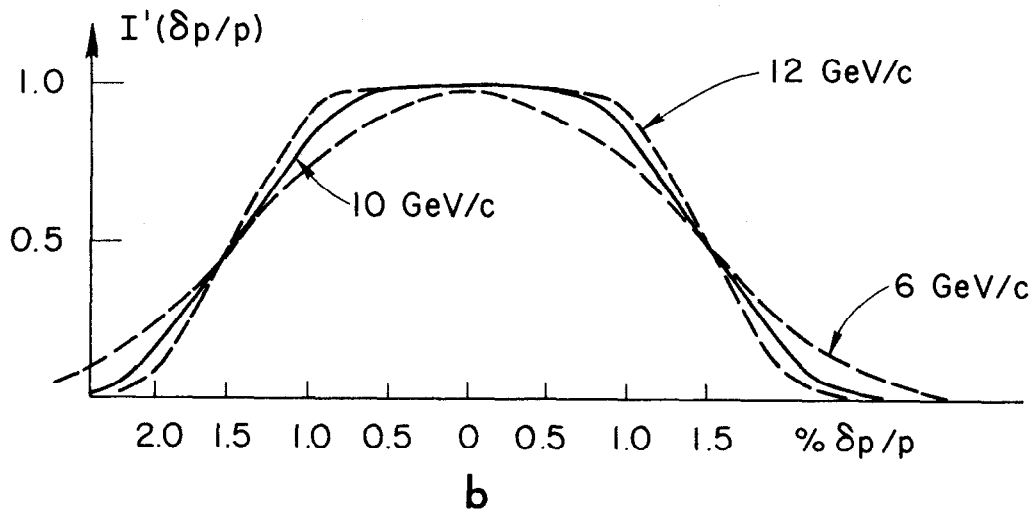
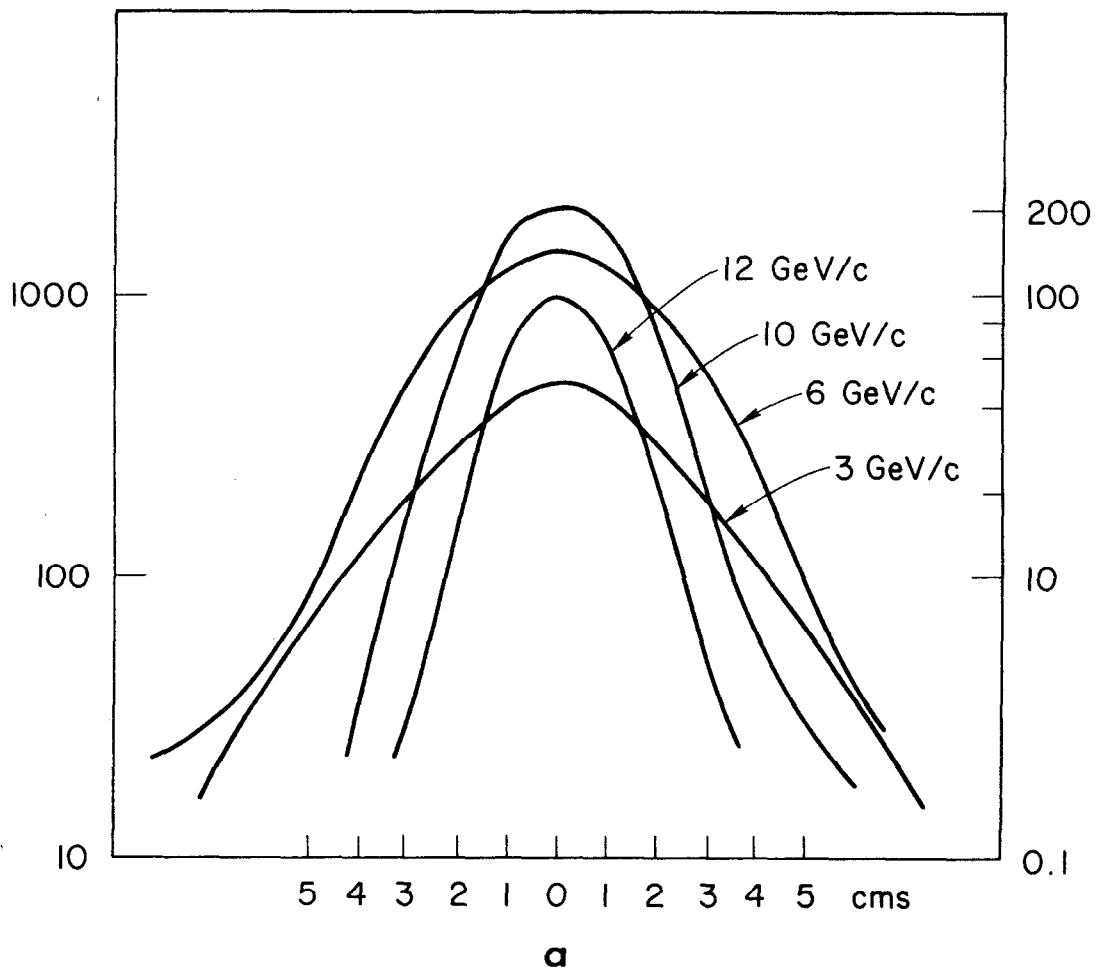


Fig. 7

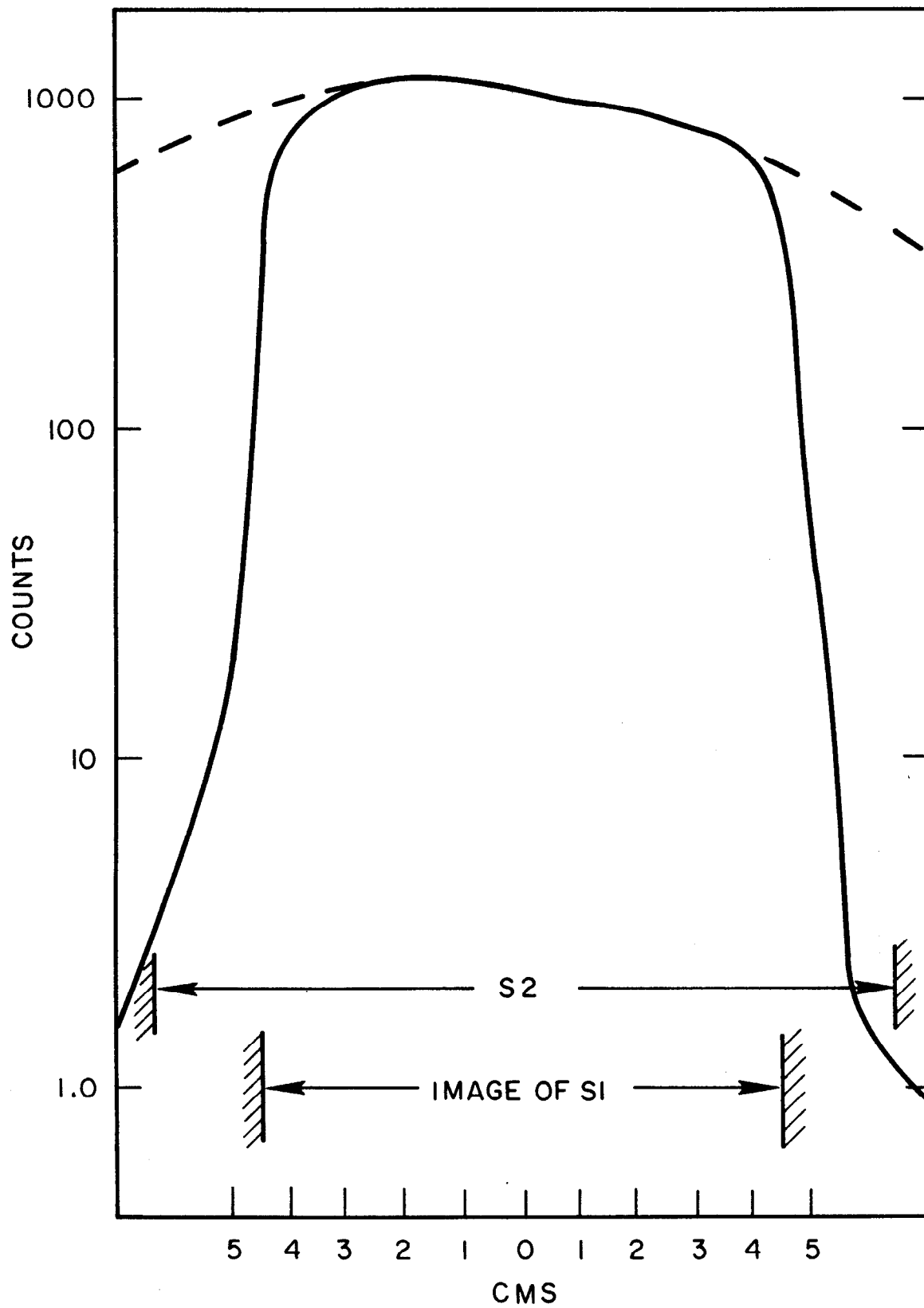


Fig. 8

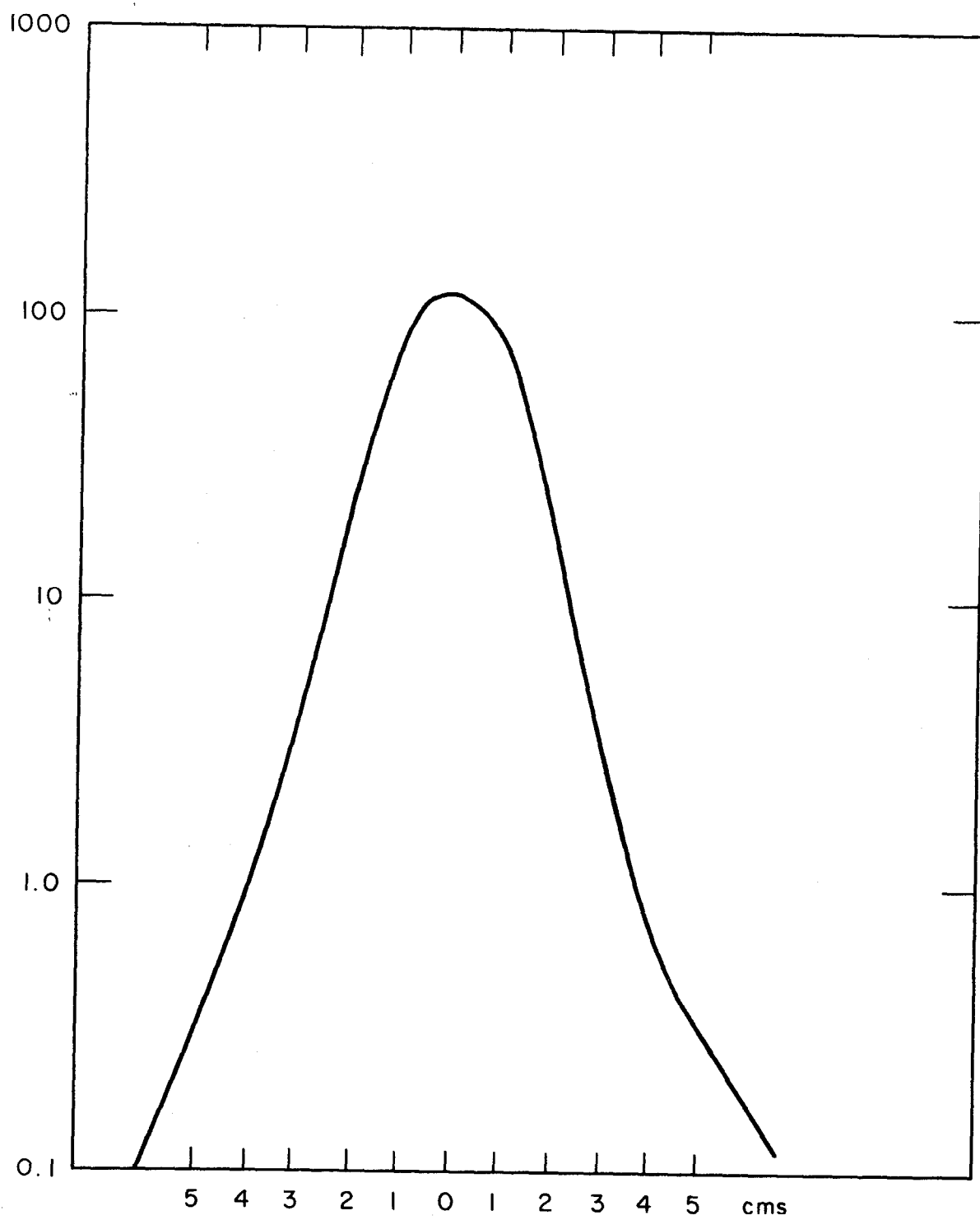


Fig. 9a

1049BII

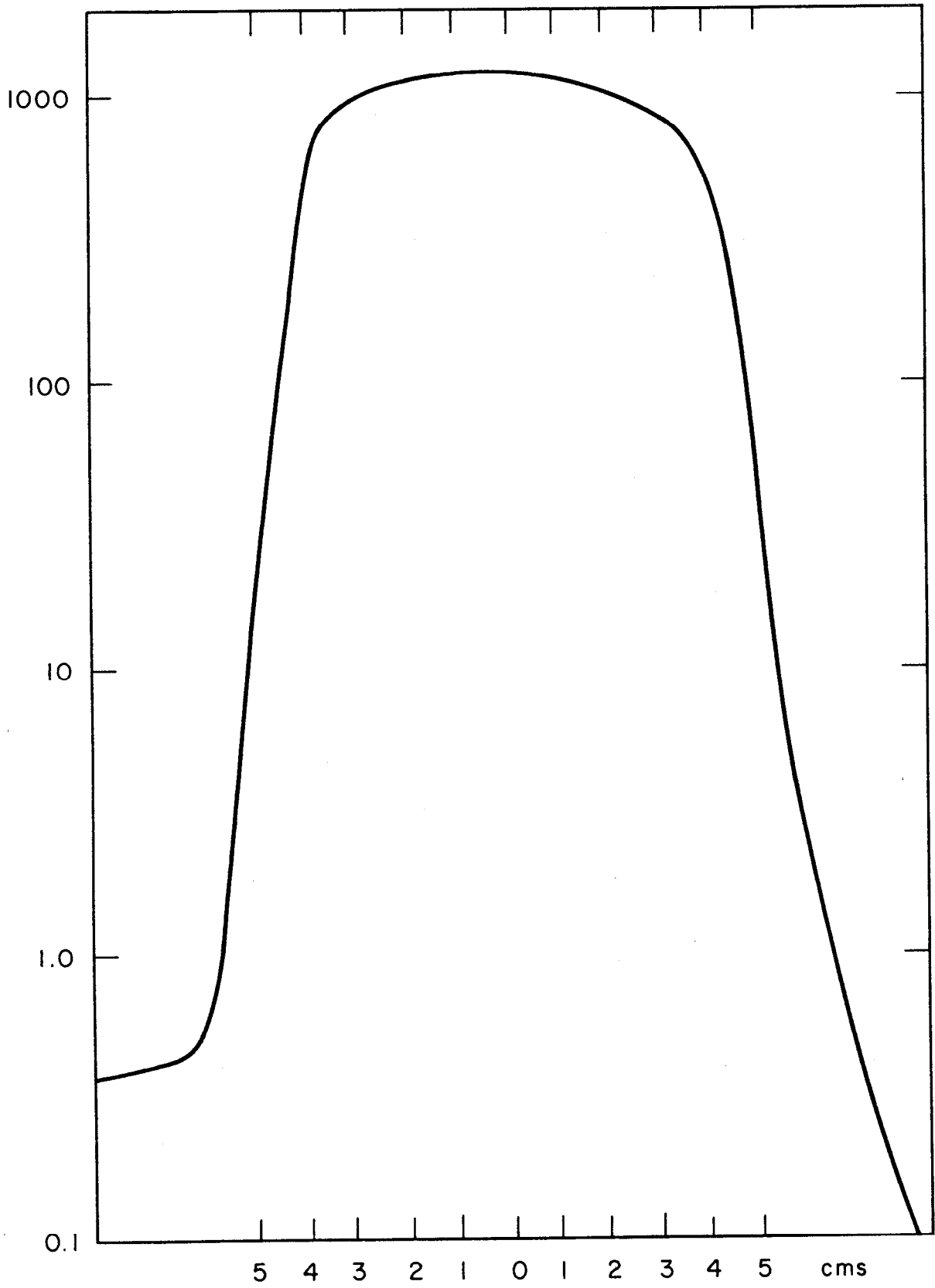
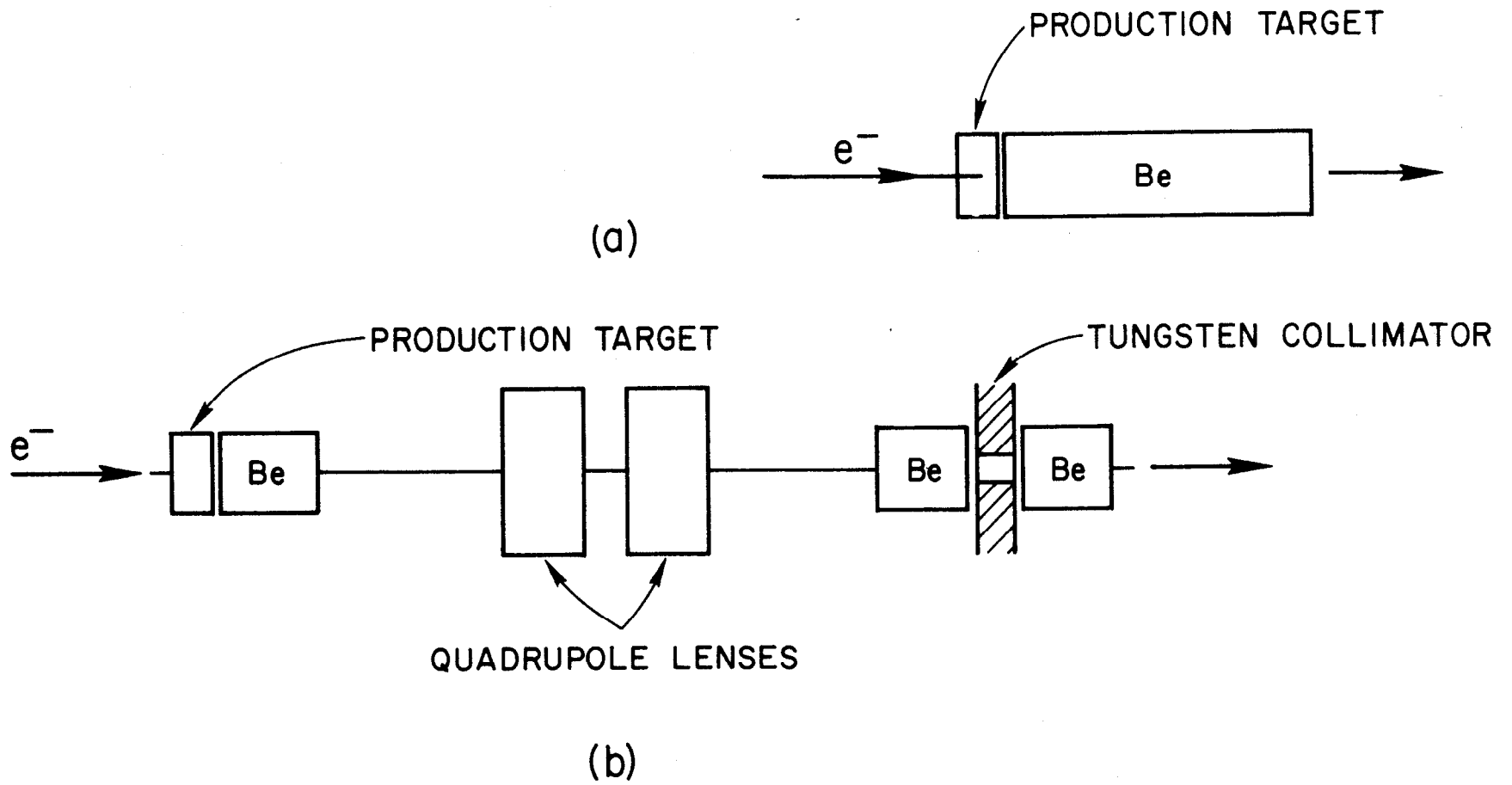


Fig. 9b



1049A7

Fig. 10